Bioconjugate Chemistry

Article

pubs.acs.org/bc

MagRET Nanoparticles: An Iron Oxide Nanocomposite Platform for Gene Silencing from MicroRNAs to Long Noncoding RNAs

E. Lellouche,[†,§,#] L. L. Israel,[‡,§,#] M. Bechor,[†,§] S. Attal,[†,§] E. Kurlander,[†,§] V. A. Asher,[†,§] A. Dolitzky,[†,§] L. Shaham,[†,∥] S. Izraeli,[∥,⊥] J.-P. Lellouche,*[,‡,§] and S. Michaeli*[,†,§]

[†]The Mina and Everard Goodman Faculty of Life Sciences, [‡]Department of Chemistry Faculty of Exact Sciences, and [§]Institute of Nanotechnology & Advanced Materials, Bar-Ilan University, Ramat-Gan 5290002, Israel

[∥]Cancer Research Center, Sheba Medical Center, Ramat Gan 5262100, Israel

[⊥]Department of Human Molecular Genetics and Biochemistry, Sackler Faculty of Medicine, Tel Aviv 69978, Israel

S *Supporting Information*

ABSTRACT: Silencing of RNA to knock down genes is currently one of the top priorities in gene therapies for cancer. However, to become practical the obstacle of RNA delivery needs to be solved. In this study, we used innovative maghemite (γ-Fe_2O_3) nanoparticles, termed magnetic reagent for efficient transfection (MagRET), which are composed of a maghemite core that is surface-doped by lanthanide $Ce^{3/4+}$ cations using sonochemistry. Thereafter, a polycationic polyethylenimine (PEI) polymer phase is bound to the maghemite core via coordinative chemistry enabled by the $[CeL_n]^{3/4+}$cations/complex. PEI oxidation was used to mitigate the in vivo toxicity. Using this approach, silencing of 80−100% was observed for mRNAs, microRNAs, and lncRNA in a variety of cancer cells. MagRET NPs are advantageous in hard to transfect leukemias. This versatile nanoscale carrier can silence all known types of RNAs and these MagRET NPs with oxidized PEI are not lethal upon injection, thus holding promise for therapeutic applications, as a theranostic tool.

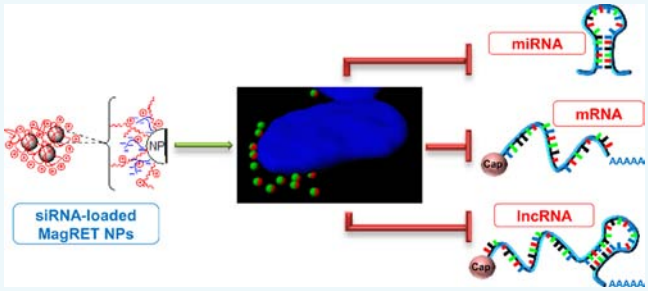

INTRODUCTION

RNA interference (RNAi) is a highly efficient regulatory process that is triggered by double-stranded RNA (dsRNA), causing gene silencing in most eukaryotes.[1] However, despite the high potential therapeutic benefits of siRNAs, such therapies are not yet available in the clinic. Several limitations exist in developing siRNAs as drugs. First, due to their large molecular weight, negative charge, and hydrophilic nature, siRNAs are unable to enter cells. Second, intravenously injected siRNA molecules are rapidly degraded by endonucleases, and excreted by renal clearance.[1] These obstacles may be overcome by utilizing nanocarriers that protect siRNA species from degradation as well as avoiding their renal excretion. Such nanocarriers include cyclodextrin polymers, lipid-based carriers, dendrimers, neutral and/or cationic polymers, gold and silica NPs, and carbon nanotubes (CNTs).[2] The positively charged polyethylenimine (PEI) have also been used to electrostatically bind siRNAs, taking advantage of its strong positive charge. Most importantly, PEI has a strong capacity to mediate endosomal escape by the well-known "proton sponge" effect leading to the release of siRNA molecules into the cytoplasm.[3]

In this context, superparamagnetic iron oxide nanoparticles (SPIONs) attracted great interest due to their safe toxicity profile and wide range of potential applications.[4] They include theranostics, local hyperthermia, drug delivery, cell separation, and imaging.[4] Most recently, Wu et al.[5] used arginine glycine aspartic acid (RGD)-modified poly(ethylene glycol)-grafted polyethylenimine (PEI) SPIONs (RGD-PEG-*g*-PEI-SPION) to specifically deliver siRNAs both in vitro and in vivo, resulting in a ∼70% down-regulation of the gene expression.

Noncoding RNAs constitute 98% of the human genome and were shown to be dysregulated in cancer cells.[6] Noncoding RNAs are divided into two types, small or longer RNAs (longer than 200 nt). miRNAs are 20−22 nt long and negatively regulate gene expression by binding imperfectly to the 3′ untranslated region (3′-UTR) of target mRNAs leading mainly to degradation of mRNAs, but also directly affect translation.[7] More than 2600 unique mature miRNAs exist in the human genome and 60% of human protein genes are regulated by miRNAs.[8] Many miRNAs are known to be oncogenic and thus are attractive targets for gene silencing therapies and for diagnosis.[9] Indeed, antisense microRNAs (anti-miRs) complexed to nanoparticles were already used to silence a variety of miRNAs.[10−13]

Compared to miRNAs which regulate gene expression only post-transcriptionally, lncRNAs are involved in transcriptional,

Received: May 15, 2015
Revised: June 8, 2015
Published: June 9, 2015

DOI: 10.1021/acs.bioconjchem.5b00276
Bioconjugate Chem. 2015, 26, 1692−1701

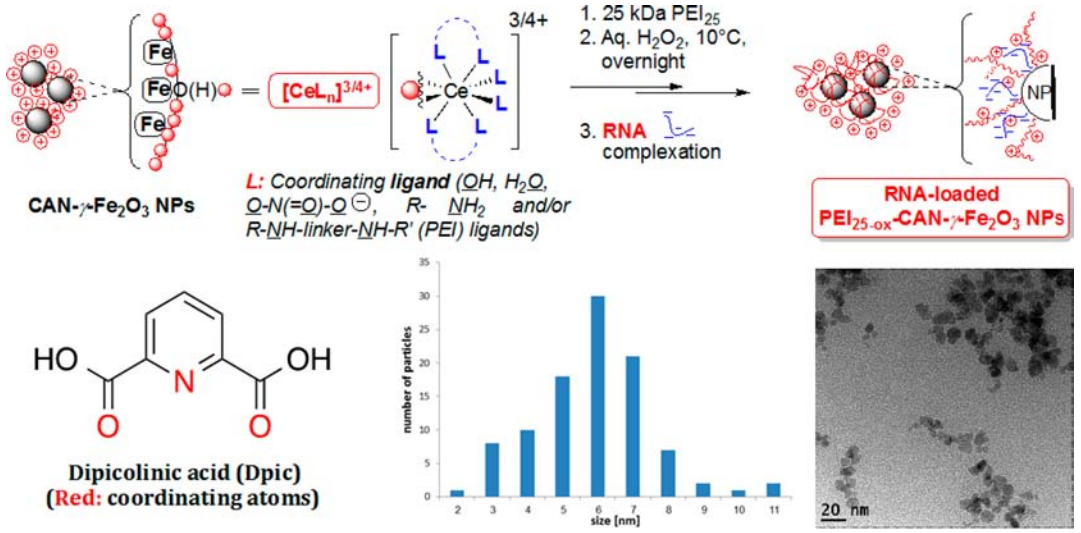

Figure 1. Two-step nanofabrication process of polycationic PEI_{25}-decorated PEI_{25}-CAN-γ-Fe_2O_3 and partially oxidized $PEI_{25\text{-}OX}$-CAN-γ-Fe_2O_3 NPs. This multiparameter optimized process includes both a critical ultrasound-assisted $[CeL_n]^{3/4+}$ complex doping step and PEI_{25} controlled low-level oxidation (aqueous H_2O_2, 10 °C, overnight) to mitigate NP toxicity. TEM analysis (scale bar: 20 nm) of final crystalline $PEI_{25\text{-}OX}$-CAN-γ-Fe_2O_3 NPs disclosed an almost spherical shape with an average NP diameter of 6.36 ± 2.65 nm (TEM measurements of more than 100 objects) with a DLS hydrodynamic diameter of 120.0 nm.

post-transcriptional, and epigenetic regulation mechanisms.[14] Recent studies reported that certain lncRNAs are dysregulated in cancers, suggesting an oncogenic-like role of these master regulators. For example, Metastasis-Associated Lung Adenocarcinoma Transcript 1 (MALAT-1) was associated with migration, invasion, metastases, and poor prognosis.[15]

In this study, we designed and tested innovative nanoscale $[CeL_n]^{3/4+}$ cation/complex-stabilized maghemite (CAN-γ-Fe_2O_3) NPs[16] as a unique potent nanoparticulate carrier system for silencing several types of RNAs. The novel nanofabrication process described here makes effective use of NP surface doping lanthanide cations/complexes ($[CeL_n]^{3/4+}$) in order to promote binding coordination of oxidized PEI. We demonstrate silencing of a variety of genes including Firefly luciferase, Matrix Metalloproteinase 14 (MMP14), and Polo-Like Kinase 1 (PLK-1). PLK-1 silencing induces G2/M arrest, caspase 3/7 activation, and PARP1 cleavage leading to apoptosis. Moreover, silencing is reported for microRNAs, including mir-21, mir-99a, and mir-486, and for the lncRNA, MALAT-1. In addition, MagRET NPs showed high gene silencing efficacy in a variety of cancer cells including hard-to-transfect human leukemia cells. Furthermore, intravenous (IV) injection of MagRET NPs to mice was not lethal at a dose of 2 mg siRNA/kg. This is the first reported nanocarrier that can efficiently silence both nuclear and cytoplasmic coding and noncoding RNAs, providing an attractive and challenging future theranostic reagent.

RESULTS

Fabrication and Characterization of MagRET NPs. The MagRET NPs were fabricated based on functional magnetic iron oxide (maghemite) nanoscale particulate systems, which were previously described.[16,17] To bypass the organic and inorganic modes of aggregation control/surface functionalization of iron oxide (magnetite and maghemite) NPs, we used a high-power ultrasound-assisted oxidative process involving the strong oxidant Ceric Ammonium Nitrate (CAN, Ce-$(NH_4)_2(NO_3)_6$). Using high-power ultrasonication, preformed brilliant black partially aggregated 10.0−15.0-nm-sized Massart magnetite (Fe_3O_4) NPs[18] were converted into brown non-aggregated hydrophilic $[CeL_n]^{3/4+}$ metal cation/complex-doped superparamagnetic maghemite (γ-Fe_2O_3) NPs (CAN-γ-Fe_2O_3 NPs) with a size of 7.61 ± 2.33 nm, determined by TEM, and 50.0 nm as determined by DLS. The NPs possess exceptional positive ζ potential values of +40.0−43.0 mV, explaining their observed NP colloidal stability in aqueous media, i.e., indicating strong repulsive interactions between highly positively charged NPs. Next, the positively charged PEI_{25} polymer was conjugated via chelation onto the surface of the CAN-γ-Fe_2O_3 NPs to obtain ultrasmall PEI_{25}-decorated PEI_{25}-CAN-γ-Fe_2O_3 NPs with a size of 6.50 ± 2.15 nm by TEM and 65.0−78.0 nm by DLS (PDI: 0.18−0.207), and a ζ potential value of +18.4 mV (optimal PEI/Fe Wt ratio: 5.25) (Figure 1).[19] A simple "saturation" experiment was performed to validate this innovative NP surface engineering based on the coordinative attachment of organic polymers to the doped $[CeL_n]^{3/4+}$ metal cations/complexes. CAN-γ-Fe_2O_3 NPs have been first reacted with a specific tridentate dipicolinic acid ligand (Dpic, Figure 1) in excess to form Dpic-modified CAN-γ-Fe_2O_3 NPs (ζ potential: +34.2 ± 0.61 mV and DLS size: 64.41 ± 0.25 nm). Importantly, this tridentate (red coordinating (H)O/C═O/N atoms, Figure 1) Dpic ligand is known to strongly chelate $Ce^{3/4+}$ cations[20−22] potentially preventing the coordinative attachment of any other interacting organic species or polymers, such as PEI_{25}. Thus, Dpic-modified CAN-γ-Fe_2O_3 NPs have been similarly reacted with a known excess amount of fluorescent FITC-labeled PEI_{25} polymer[23] followed by extensive NP cleaning. The Dpic coordinative attachment onto the surface of reactive CAN-maghemite NPs was confirmed using FTIR (Supporting Information Figure S2 for detailed spectra). Comparison of both FTIR spectra of starting CAN-maghemite NPs and of Dpic-decorated ones, unambiguously proved the presence of the NPs surface-complexed organic Dpic ligand. Indeed, several absorption peaks characteristic of Dpic functionalities might be readily identified. For example, peaks appearing at 807 (medium) and 1578−9

DOI: 10.1021/acs.bioconjchem.5b00276
Bioconjugate Chem. 2015, 26, 1692−1701

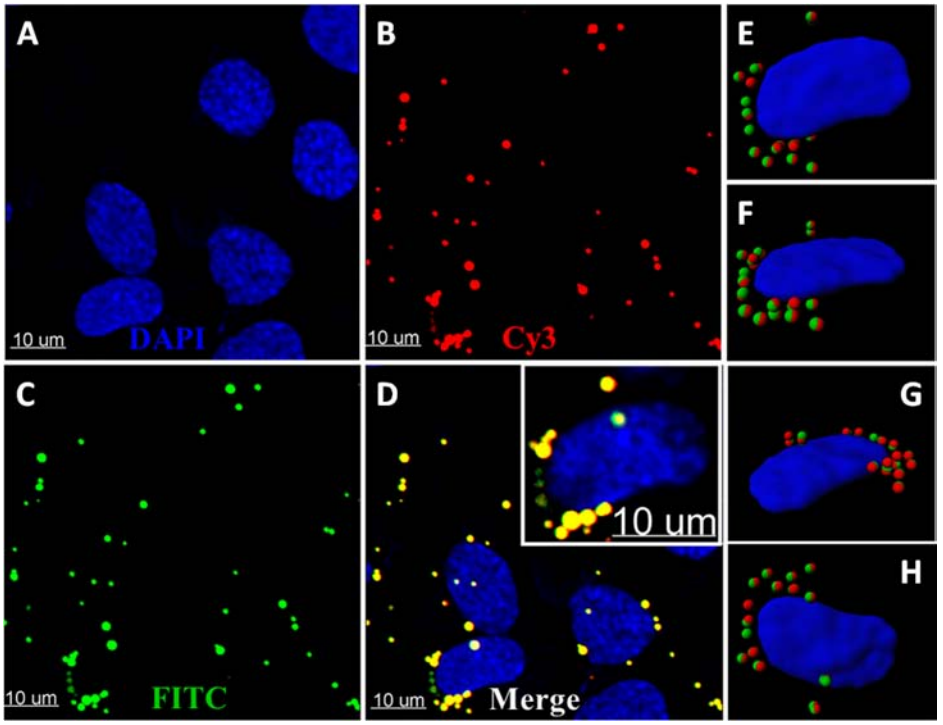

Figure 2. Penetration of MagRET NPs to SK-OV-3 cells. SK-OV-3 cells (15×10^4 cells/well) were transfected with siGLO Green Transfection Indicator (50 nM) (FITC) (C) mixed with MagRET NPs at a 0.315 Fe/siRNA w/w ratio. After 24 h, lysosomes were stained with Lysotracker (Cy3) (B), cells were fixed, and nuclei were stained with DAPI (blue) (A). Images were taken with a Leica TCS SPE (63×) confocal laser scanning microscope (CLSM) (A–D), and then the 3D images were edited using Imaris software (Bitplane) (E–-H).

(medium) cm^{-1} characterized both aromatics C—H "oop" and C═C (in-ring) stretchings, respectively. In addition, both 1041–2 cm^{-1} (broad and strong), and 1260 cm^{-1} (strong and sharp) peaks related to C—O (carboxylic acid/ester) stretchings. Moreover, the new medium-sized peak appearing at 1719 cm^{-1} characterized carboxylic acids C═O stretchings. Finally, broad 2985 and 3081 cm^{-1}-centered peaks might be readily assigned to carboxylic acids O—H and aromatics C—H stretchings, respectively.

Then, the fluorescence of the washing phase was measured and found to exactly fit the initial amount of FITC-PEI_{25} engaged in this "surface saturation" experiment.[24] Therefore, we might conclude without ambiguity that the FITC-PEI_{25} polymer phase was unable to bind Dpic-modified CAN-γ-Fe_2O_3 NPs most likely because of the first step formation of "saturated" [$Ce^{3/4+}$-$Dpic_3$] complexes.

Finally and in a second step, to mitigate the expected in vivo toxicity of PEI_{25}[25] a simple controlled oxidative process of the PEI_{25} shell was performed using aqueous H_2O_2. These resulting oxidized $PEI_{25\text{-}ox}$-CAN-γ-Fe_2O_3 NPs were further characterized and shown to possess average TEM and DLS sizes of 6.36 ± 2.65 and 120.0 nm, respectively, and a ζ potential value of +29.4 mV.

In order to identify the structural chemical modifications following this oxidation process, three separate oxidation reactions of the sole PEI_{25} phase have been conducted at increasing aqueous H_2O_2 levels and analyzed by FTIR spectroscopy. Since the controlled H_2O_2-mediated oxidation of intermediate PEI_{25}-CAN-γ-Fe_2O_3 NPs has been done at a very low level (0.1% molar H_2O_2), PEI_{25} oxidation reactions have been set up with oxidation levels of 0.1%, 1.0%, and 5.0%. Then, the resulting oxidized PEI_{25} products were checked for functionality by FTIR spectroscopy. Figure S3 (Supporting Information) shows all significant FTIR spectra of starting PEI_{25} (red), 0.1% oxidized PEI_{25} (blue), 1.0% oxidized PEI_{25} (teal), and 5.0% oxidized PEI_{25} (black). All three oxidized PEI_{25} phase FTIR spectra clearly disclose significant absorption peak changes relating to the formation of *N*-relating oxidized species in the 1313.88–1686.81 cm^{-1} frequency range. For example, specific strong peaks appear at 1660.69 (5.0%), 1686.31 (1.0%), and 1686.81 (0.1%) cm^{-1} that are characteristic of C═N oxime bond (C═N—OH) stretchings, while such peaks are absent in the spectrum of nonoxidized PEI_{25}. In addition, newly formed alkane nitro groups (-NO_2) can be clearly identified that exhibit both characteristic asymmetric (1476.78 (0.1%)/1473.84 (1.0%)/1475.49 (5.0%) cm^{-1}) and symmetric (1315.92 (0.1%)/1313.88 (1.0%)/1311.97 (5.0%) cm^{-1}) stretchings. Moreover, all the strong absorption peaks appearing at 1551.97–1594.77 (0.1%)/1559.14–1594.53 (1.0%)/1569.04–1594.73 (5.0%) cm^{-1} are also quite characteristics of N═O nitroso bond stretchings.

Efficient Silencing Using MagRET NPs with Minor Cellular Toxicity. As a first step for utilizing MagRET NPs for gene silencing, siRNA binding to the NPs was examined and efficient binding was observed (Supporting Information Figure S1). Next, the entry of MagRET NPs to cells was examined in SK-OV-3 cells using NPs bound to FITC-labeled siRNAs (green) (Figure 2C). NPs were traced with respect to the lysosomes (red) (Figure 2B), the end point of the endocytic pathway. As expected, and in accordance with the literature,[1] MagRET NPs penetrated SK-OV-3 cells via the endocytic pathway and reached the lysosomes since a colocalization can be seen between the FITC and Cy3 fluorescence (Figure 2D–H).

Next, to determine whether MagRET NPs can efficiently silence genes, we used a two-gene reporter system based on the

DOI: 10.1021/acs.bioconjchem.5b00276
Bioconjugate Chem. 2015, 26, 1692–1701

Firefly and *Renilla* genes, stably expressed in U2OS cells. Specific silencing (*Firefly*) is measured, while the *Renilla* was used as a control for cell viability. *Firefly* luciferase silencing was conducted using a constant amount of siRNA (100 nM which is equal to ∼0.166 μg of siRNA) mixed with MagRET NPs using different Fe/siRNA w/w ratios (0.063−0.63) corresponding to iron (Fe) concentrations of 0.1−1 μg/mL (Figure 3A).

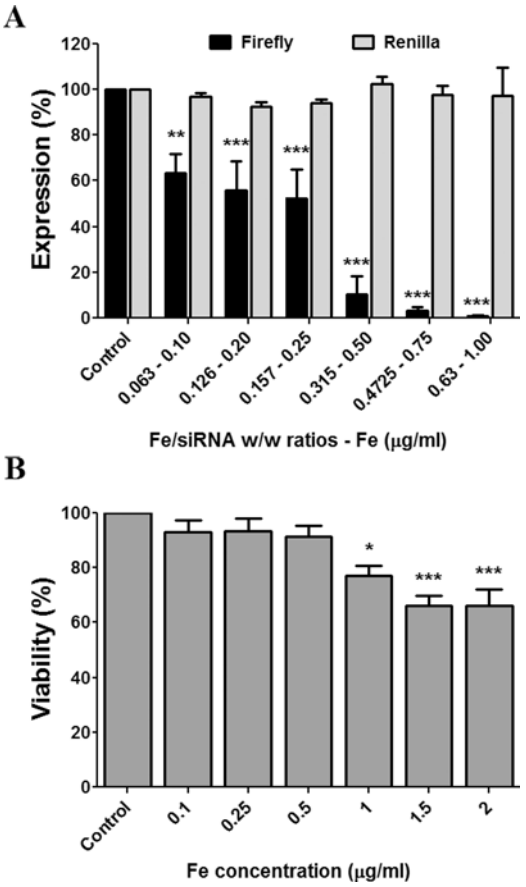

Figure 3. Luciferase silencing with MagRET NPs in U2OS-Luc cells and toxicity by MTT in BxPC-3 cells. (A) U2OS-Luc cells (1×10^4 cells/well) were transfected with Firefly luciferase siRNA (0.166 μg) (100 nM) mixed with MagRET NPs at different Fe/siRNA w/w ratios or without NPs (control). After 48 h, cells were assayed for both Firefly and *Renilla* luciferase activities using Dual-GLO Luciferase Assay System. Silencing efficacy is denoted by luciferase activity normalized to control luciferase activity. Data are expressed as mean ± SEM of three different experiments according to the results of a Two Way ANOVA with multiple comparison Bonferroni post hoc analysis (**$p < 0.01$, ***$p < 0.001$ vs control Firefly). (B) BxPC-3 cells (2×10^4 cells/well) were treated with different concentrations of iron (Fe) or without NPs (control). After 72 h, medium was removed and replaced with fresh medium containing MTT. The adsorption values were measured at 570 nm and normalized to the control sample. Data are expressed as mean ± SEM of five different experiments based on a One Way ANOVA with multiple comparison Bonferroni post hoc analysis (*$p < 0.05$ and ***$p < 0.001$ vs control).

Knockdown of 89 ± 8% silencing was observed even at a low Fe/siRNA ratio of 0.315, and in the same time no changes in the *Renilla* levels were observed, indicating that no toxicity was induced. Significant silencing of 36 ± 8% to 47 ± 12% with lower Fe/siRNA w/w ratios (0.063 to 0.157, respectively) was also achieved, indicating that the limiting factor is the amount of NPs.

Several studies reported that exposure to SPIONs is associated with significant toxic effects depending on their surface coating nature.[4] In addition, PEI is known to induce cytotoxicity by disrupting the cell membrane, leading to necrotic cell death.[26]

To further investigate if MagRET NPs are toxic, we treated BxPC-3 cells with increasing amounts of iron (Fe) (0.1−2 μg/mL) (Figure 3B). Mitochondrial activity was measured using the MTT assay. Even after 72 h, no significant changes in cell proliferation and viability were observed following NP treatment at concentrations up to 0.5 μg/mL. However, higher concentrations of MagRET NPs resulted in moderate (23 ± 3% to 34 ± 6%) toxicity. The results indicate no adverse toxicity using a Fe/siRNA ratio optimal for silencing in the dual luciferase system.

Silencing of MMP1-14 and PLK-1 with MagRET NPs in a Variety of Cancer Cells. The Dual-Luciferase reporter assay described above is quick and efficient, but is excessively sensitive. We therefore explored the silencing of authentic highly expressed genes in a variety of cancer cells.

Matrix metalloproteinases are of great interest since many of these proteins are overexpressed in a wide range of human cancers. For example, MMP14 (MT1-MMP), a primary interstitial collagenase, is overexpressed in pancreatic cancer cells and metastatic lesions,[27] and in addition, MMP14 was shown to be involved in chemoresistance to the drug, gemcitabine.[28]

MMP14 was silenced in BxPC-3 cells. Based on the data obtained with the Dual-Luciferase assay, we used a Fe/siRNA w/w ratio of 0.315 as optimal for silencing. As can be seen in Figure 4B, a statistically significant depletion of the protein was observed as the result of silencing (Figure 4A). Depletion of 84 ± 10% was observed following silencing with MMP14 specific siRNA, but not with nonspecific siRNAs, indicating the silencing can also be achieved for highly expressed genes.

To further investigate whether silencing using MagRET NPs can generate a biological phenotype, the PLK-1 kinase was silenced. PLK-1 is highly expressed in a large number of cancer cells and plays a key role in cell cycle progression. It has been previously shown that PLK-1 silencing results in cell cycle arrest at G2/M as well as chemotherapy resistance.[29]

SK-OV-3 cells were transfected with PLK-1-specific siRNAs complexed to MagRET NPs, and PLK-1 mRNA expression was evaluated in parallel to cell cycle analysis. A significant knockdown of 85 ± 3% was observed by real-time PCR following PLK-1 silencing (Figure 5A). Silencing induced major cell cycle arrest at the G2/M phase (from 10.5 ± 1.6% to 56 ± 4%), a decrease in cell percentage in the G0/G1 phase (from 73 ± 3% to 29 ± 4%), and more importantly, a significant increase in the Sub-G1 phase from 2.5 ± 0.8 to 15 ± 3% (Figure 5B).

Caspase 3 and 7 play a key role in apoptosis.[30] PLK-1 silencing using MagRET NPs induced apoptosis in SK-OV-3 cells, manifested by a significant induction of 57 ± 5% in caspase 3/7 activities following silencing of PLK-1 with a siRNA concentration of 100 nM. However, no significant induction was observed with a concentration of 50 nM (Figure 5D). Moreover, we analyzed the specific cleavage of the poly(ADP-ribose) polymerase 1 (PARP1), which is involved in DNA repair processes under cellular stress. Severe cell damage results in caspase 3 activation and specific cleavage of PARP1.[31]

DOI: 10.1021/acs.bioconjchem.5b00276
Bioconjugate Chem. 2015, 26, 1692−1701

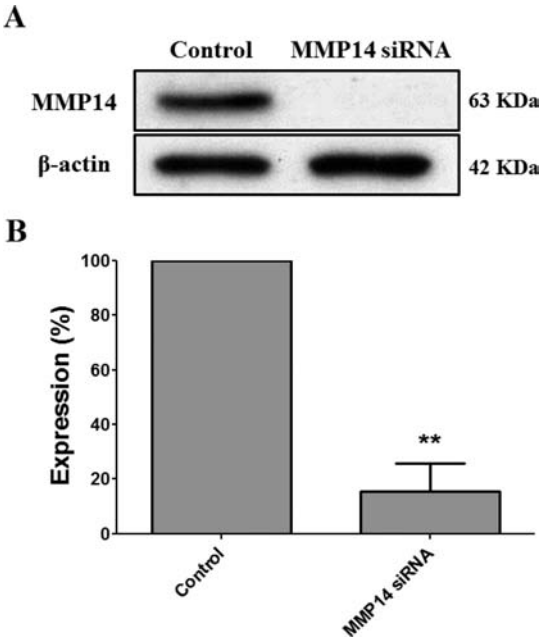

Figure 4. MMP14 silencing in BxPC-3 cells. BxPC-3 cells (6×10^5 cells/well) were transfected with MMP14 specific siRNA (100 nM) or nonspecific siRNA (100 nM) (control) mixed with MagRET NPs at a 0.315 Fe/siRNA w/w ratio. After 48 h, proteins were extracted and the level of silencing was analyzed by (A) Western blot analysis (data are representative of three independent experiments) and (B) MMP14 levels were quantified with *ImageJ* software (β-actin was used as a loading control). Data are expressed as mean ± SEM of three different experiments according to the results of a One-Sample *t* test to compare silencing to the normalized control group (**$p < 0.01$).

Indeed, silencing of PLK-1 in SK-OV-3 cells resulted in the cleavage of the PARP1 protein (Figure 5C).

These results demonstrate that MagRET NPs complexed with gene-specific siRNAs can induce significant reduction in target mRNA and protein levels leading to biological clear phenotypes.

Silencing by MagRET NPs of microRNA and lncRNAs in Cancer Cells and Hard-to-Transfect Leukemia Cells. Hard-to-transfect cells, such as primary, nondividing, and cells in suspension, are resistant to transfection by conventional approaches such as commercial liposomes.[32] So far, siRNA delivery to cells in suspension can be achieved almost exclusively by electroporation which is expensive, cytotoxic, and cannot be considered for in vivo applications.[32]

CMK cells were established from a Down's syndrome patient with acute megakaryoblastic leukemia.[33] Transfection of CMK cells is difficult and we therefore examined the potential of MagRET NPs to silence microRNAs in these cells. The results (Figure 6B and C) show 95 ± 3% reduction in the level of mir-99a, and 90 ± 8% reduction in the level of mir-486 using a miRNA inhibitor concentration of 25 and 50 nM, respectively.

Mir-21 is one of the most extensively documented miRNA overexpressed in a variety of cancer cells, and involved in tumor progression metastases and resistance to chemotherapy.[34] Thus, mir-21 is considered a very promising therapeutic target for cancer. Transfection of BxPC-3 cells with MagRET NPs complexed with a mir-21 inhibitor led to a significant down-regulation of 89 ± 5% at a concentration of 100 nM (Figure 6A).

LncRNA MALAT-1, one of the most abundant lncRNA species, is aberrantly up-regulated during metastasis of nonsmall cell lung cancer, and acts as early prognostic marker for poor survival.[35] MALAT-1 was previously silenced with the commercial Lipofectamine 2000 reagent,[36] but silencing of lncRNA with nanocarriers has not been reported. MALAT-1 is a nuclear lncRNA and is localized in nuclear speckles together with splicing factors.[37] Although MagRET NPs are too big to penetrate the cell nucleus as can be seen in Figure 2, MagRET NPs can induce MALAT-1 silencing with the same efficiency as the commercial Lipofectamine 2000 reagent (Figure 6D).

Thus, MagRET NPs are capable of efficiently silencing small and long noncoding RNAs that reside in either the cytoplasm or nucleus in a variety of cancer cells.

Lack of MagRET NP Toxicity Following in Vivo Treatment. Following intravenous injection, PEI can cause severe damage. This toxicity is due to the fact that PEI, a very positively charged polymer, can interact with negatively charged membranes of red blood cells (RBCs). This interaction causes RBC aggregation and lysis, leading to thrombosis, and finally, to animal death.[7]

One way to mitigate the toxicity is the chemical modification of the primary amines of the PEI. We suggested that mild oxidation could modify part of the primary amines changing the surface properties of the NPs with only minor changes to the silencing capabilities of the NPs. To determine if MagRET NPs can be potentially used as a therapeutic platform in vivo, we examined NPs toxicity by injecting mice with PEI-oxidized ($PEI_{25\text{-}ox}$-CAN-γ-Fe_2O_3) (MagRET NPs), PEI-unmodified (PEI_{25}-CAN-γ-Fe_2O_3), and iron core (CAN-γ-Fe_2O_3) nanoparticles, or with saline as a control (Figure 7). As expected, mice injected with unmodified PEI died within 2 h post injection, while mice injected with MagRET NPs ($PEI_{25\text{-}ox}$-CAN-γ-Fe_2O_3) survived. However, the injection of the iron core itself did not lead to death, suggesting that toxicity is due to the PEI, and mild oxidation is able to mitigate this toxic effect. Indeed, MagRET NPs complexed with siRNA at a concentration of 2 mg/kg was safely injected IV three times with an interval of 24 h (data not shown).

These results together with the very efficient in vitro silencing suggest that MagRET NPs can be potentially used as a platform for the in vivo delivery of siRNAs.

■ DISCUSSION

In this study, we describe the fabrication and use of ultrasmall maghemite nanoparticles, i.e., the MagRET NPs, surface-doped with $[CeL_n]^{3/4+}$ cations/complexes by high-power sonochemistry, enabling binding of oxidized $PEI_{25\text{-}ox}$ via coordinative chemistry. MagRET NPs are able to silence a variety of RNAs in different cancer cells including cells that are resistant to transfection. MagRET NPs do not cause mortality upon IV injection and thus can be further developed as a nanoscale platform for therapy. This is the first study demonstrating that silencing of nuclear lncRNAs can be achieved with NPs that enter the cytoplasm via the endocytic pathway.

Unique Physicochemical Properties of MagRET NPs. MagRET NPs have unique physicochemical features resulting from the optimized NP surface functionalization created by doping $[CeL_n]^{3/4+}$ metal cations/complexes (L: $Ce^{3/4+}$ cation complexing ligands, see Figure 1 for details). Indeed, $[CeL_n]^{3/4+}$ metal cations/complexes can act as strong Lewis acid centers enabling successful coordinative attachment of any Lewis base N/S/O-containing organic species via L ligand exchange.[38−42]

DOI: 10.1021/acs.bioconjchem.5b00276
Bioconjugate Chem. 2015, 26, 1692−1701

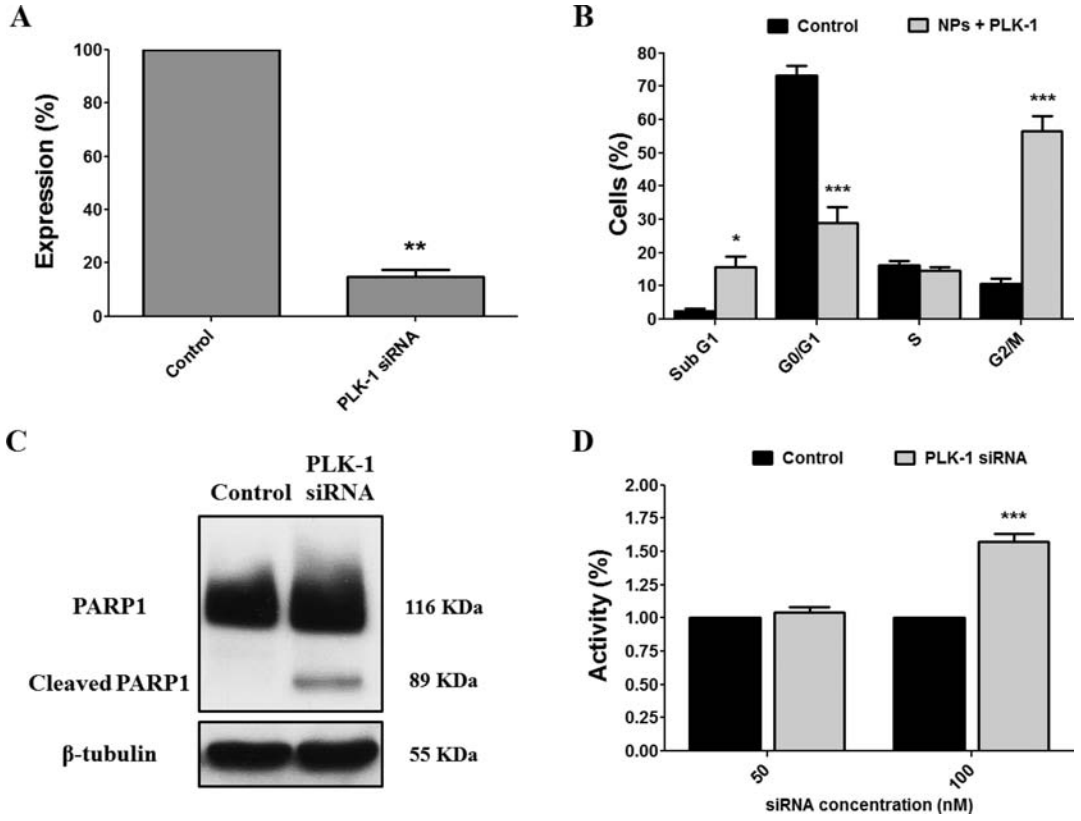

Figure 5. RT-PCR, cell cycle analysis, PARP1 cleavage, and caspase 3/7 activities in SK-OV-3 cells after PLK-1 silencing. SK-OV-3 cells (6×10^5 cells/well) were transfected with PLK-1 siRNA (200 nM) or nonspecific siRNA (control) (200 nM) mixed with MagRET NPs at a 0.315 Fe/siRNA w/w ratio. After 48 h, total RNA, proteins and cells were collected. (A) Level of PLK-1 mRNA was analyzed by real-time RT-PCR. Data are expressed as mean ± SEM of three different experiments according to a One-Sample *t* test results to compare silencing to the normalized control group (**$p < 0.01$). (B) Cells were collected, fixed, stained with PI solution and DNA content was analyzed by flow cytometry. Data are expressed as mean ± SEM of three different experiments according to a Two Way ANOVA with multiple comparison Bonferroni post hoc to compare percent of cells from control and PLK-1 siRNA groups (**$p < 0.01$, ***$p < 0.001$). (C) PARP1 cleavage was assayed by Western blot analysis (data are representative of three independent experiments). (D) SK-OV-3 cells (1×10^4 cells/well) were transfected with PLK-1 siRNA (50 or 100 nM) or nonspecific siRNA (control) (50 or 100 nM) mixed with MagRET NPs at a 0.315 Fe/siRNA w/w ratio. After 48 h, cells were assayed for caspase 3/7 activities using the Caspase-Glo 3/7 Assay system. Caspase 3/7 activities are represented by caspase 3/7 activities after silencing, normalized to nonspecific caspase 3/7 activities. Data are expressed as mean ± SEM of three different experiments according to the results of a Two Way ANOVA with multiple comparison Bonferroni post hoc analysis (***$p < 0.001$ vs control).

Therefore, via the coordinative chemistry of corresponding $[CeL_n]^{3/4+}$ cations, we were able to successfully link PEI_{25}/$PEI_{25\text{-}ox}$ phases without the need for any bifunctional linker.

Another unique feature of MagRET NPs is the controlled oxidation of the NP PEI_{25} shell. During oxidation, the original PEI_{25} component undergoes several types of chemical modification, leading to the formation of mixed primary neutral and/or amphoteric hydroxylamines (−NH−OH)/nitroso species (−N═O)/nitro species (−N(+)(═O)O(−)), secondary hydroxylamines (−R(R′)N−OH), and tertiary *N*-oxides ($R_3N(+)-O(-)$) within the oxidized $PEI_{25\text{-}ox}$ phase. Indeed, we found that all these suspected structural modifications caused by this special oxidation step have been successfully identified by FTIR spectroscopy even at the lowest oxidation level of 0.1% molar H_2O_2.

The increased positive potential of the $PEI_{25\text{-}ox}$-CAN-γ-Fe_2O_3 NPs (MagRET NPs) might arise from the fact that PEI_{25} oxygenated oxidized amine species have a thermodynamically stronger O-relating Lewis base character (hardness) than nonoxidized related amine groups,[40−42] resulting in more effective O (PEI_{25ox}) vs N (PEI_{25})-based competitive coordinative covalent interactions within NP surface cationic $[CeL_n]^{3/4+}$ complexes, which then affects shell internal rearrangements on the NP surface. The oxidation affinities of PEI_{25} primary, secondary, and tertiary amine group subpopulations leads to differential surface charge modifications of the NP outer layer that is exemplified by the ζ potential. Interestingly, this is the first time that a controlled H_2O_2-mediated oxidation of a NP-linked polycationic polymeric PEI_{25} shell has been successfully implemented and optimized to chemically modify the accessible types of PEI_{25} primary, secondary, and tertiary amine groups at a minimal level.

Oxidized PEI Compared to Other PEI Modifications to Mitigate Toxicity. PEI was found to be toxic, preventing its use in in vivo applications. Different approaches were considered to modify the original PEI polymers in order to mitigate the toxicity, such as conjugation of different molecules, including polysaccharides, hydrophobic moieties, as well as poly(ethylene glycol) (PEG).[25] The conjugation of such molecules can potentially affect the NP size which is one of the most important limiting factors for NPs to penetrate tumors via the enhanced permeability and retention (EPR) effect.[7] In this study, we successfully mitigated the in vivo toxicity of PEI_{25}-unmodified (PEI_{25}-CAN-γ-Fe_2O_3) NPs by the

DOI: 10.1021/acs.bioconjchem.5b00276
Bioconjugate Chem. 2015, 26, 1692−1701

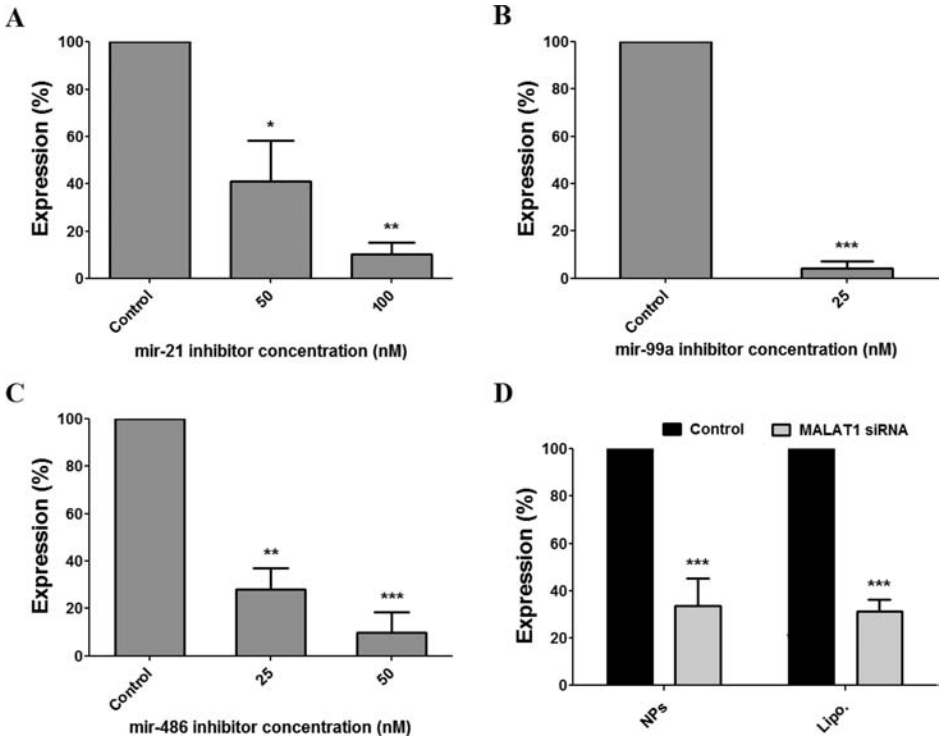

Figure 6. Noncoding RNA silencing in a variety of cancer cells including hard-to-transfect cells. (A) BxPC-3 cells (3×10^5 cells/well) were transfected with mir-21 inhibitor (50 or 100 nM) or negative control (control) (100 nM) mixed with MagRET NPs at a 0.315 Fe/siRNA w/w ratio. After 48 h, levels of mir-21 miRNA were analyzed by real-time RT-PCR. Data are expressed as mean ± SEM of three different experiments according to the results of a One Way ANOVA with multiple comparison Bonferroni post hoc analysis ($*p < 0.05$ and $**p < 0.01$ vs control). (B,C) CMK cells (25×10^4 cells/well) were transfected with (B) mir-99a (25 nM) or (C) mir-486 inhibitors (25 and 50 nM) or negative control (25 or 50 nM, respectively) complexed with MagRET NPs with a 0.315 Fe/siRNA w/w ratio. After 48 h, levels of mir-99a and mir-486 miRNAs were analyzed by real-time RT-PCR. For mir-99a, data are expressed as mean ± SEM of three different experiments according to the results of a One-Sample *t* test to compare silencing to normalized control group ($***p < 0.001$). For mir-486, data are expressed as mean ± SEM of three different experiments according to the results of a One Way ANOVA with multiple comparison Bonferroni post hoc analysis ($***p < 0.001$ vs control). (D) U2OS cells (6×10^5cells/well) were transfected with MALAT-1 siRNA (150 nM) or nonspecific siRNAs (150 nM) (control) complexed with MagRET NPs with a 0.315 Fe/siRNA w/w ratio or with Lipofectamine 2000 reagent (Lipo.). After 48 h, the level of MALAT-1 was analyzed by real-time RT-PCR. Data are expressed as mean ± SEM of three different experiments according to the results of a Two Way ANOVA with multiple comparison Bonferroni post hoc analysis ($***p < 0.001$ vs control).

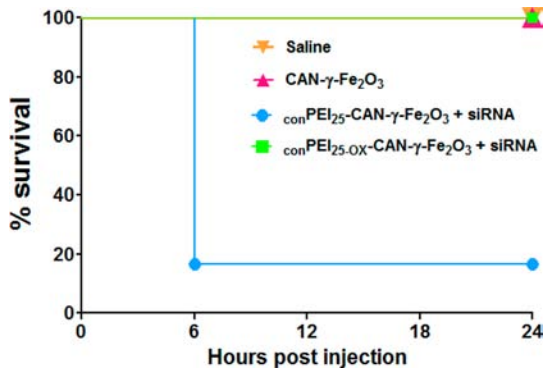

Figure 7. Mortality after IV injection of different CAN-γ-Fe_2O_3 NPs. BALB/c mice were injected intravenously with CAN-γ-Fe_2O_3 (0.315 mg/kg), PEI_{25}-CAN-γ-Fe_2O_3 (0.315 mg/kg), or $PEI_{25\text{-}OX}$-CAN-γ-Fe_2O_3 (MagRET) NPs (0.315 mg/kg) or saline (control). Each group was composed of six mice. Toxicity of injected NPs was determined as animal death within 24 h post injection.

controlled oxidation of the PEI_{25} amino groups. Compared to the previously described PEI modifications, this modification is simple, quick, and inexpensive, and most importantly it does not affect the particle size, as measured by TEM (Figure 1). Moreover, following oxidation, not only did we observe a decrease in the ζ potential values of MagRET NPs, but surprisingly the ζ potential increased. This unique property may explain why these NPs remained effective in silencing despite the oxidation.

MagRET NPs Silence Nuclear Genes. Since the discovery of RNAi it was assumed that silencing activity occurs in the cytoplasm. It is still unclear how RNAi can regulate transcription and splicing in mammalian cells.[43] However, siRNAs have been reported to silence 7SK and U6 snRNAs that reside exclusively in the nucleus.[44] Recent studies provide evidence that the RNAi endonuclease AGO2 is also found in the nucleus. However, the study did not detect the loading of duplex RNA in the nucleus, and other RNA-induced silencing complex (RISC)-loading factors are absent in the nucleus.[45] Our study suggests that MALAT-1 can be efficiently silenced with nanocarriers that cannot enter the nucleus because of their size (Figure 2). Thus, the silencing described here requires that the RISC assembly take place in the cytoplasm. Thus, nuclear silencing is mediated with cytoplasmically assembled RISC that most probably enters the nucleus. The mechanism by which RISC is transported to the nucleus remains enigmatic.

MagRET NPs is an Efficient Carrier for Silencing Leukemic Cells. Current gene delivery methods include viral

DOI: 10.1021/acs.bioconjchem.5b00276
Bioconjugate Chem. 2015, 26, 1692−1701

vectors and a variety of organic and inorganic carriers.[32] To date, the only way to efficiently transfect lymphoma/leukemia cells is by electroporation.[32] There is therefore an urgent need to develop additional reagents that can improve the current transfection methods. In this study, we showed that MagRET NPs not only silence mRNA and lncRNA in adherent cancer cells but can efficiently silence miRNAs, which are overexpressed in the CMK cells (Shaham and Izraeli, unpublished) (Figure 6). The ability of MagRET NPs to transfect these cells may be explained by the colloidal properties of the NPs that enable the particles to come in close contact with cell membranes even when the cells are in suspension.[3]

Thus, MagRET NPs holds the potential to become a powerful carrier for silencing genes in various cancers including leukemias using a variety of RNA targets from microRNA to lncRNAs.

■ CONCLUSIONS

In summary, we designed and fully characterized innovative nanoscale maghemite (γ-Fe_2O_3) nanoparticles, which are stabilized via a unique NP surface doping by lanthanide $Ce^{3/4+}$ cations using high-power sonochemistry. Thus, this $Ce^{3/3+}$ cation/complex functional shell has been shown to effectively promote the binding of an H_2O_2-oxidized $PEI_{25\text{-}ox}$ phase via $Ce^{3/3+}$ cation/complex-driven coordinative chemistry. These magnetic functional NPs, termed MagRET, have been shown to efficiently silence all main types of RNAs from mRNA to the noncoding RNAs miRNAs and lncRNAs. Using this approach, effective silencing of a variety of genes including Firefly luciferase and overexpressed MMP14, and PLK-1 was demonstrated. In addition, the observed potent PLK-1 silencing resulted in cell apoptosis, as evident by G2/M arrest, caspase 3/7 activation, and PARP1 cleavage. Moreover and very interestingly, MagRET NPs showed high gene silencing efficacy in hard-to-transfect human leukemia cells, which are reluctant to transfection when using conventional approaches such as commercial liposomes. Since IV injection of MagRET NPs to mice was not lethal at a therapeutic dose, these NPs hold great promise for therapeutic applications as an innovative theranostic tool.

■ MATERIALS AND METHODS

The MagRET NPs used in these RNA delivery and gene silencing experiments were prepared in a two-step nanofabrication process that included (i) decoration of $[CeL_n]^{3/4+}$-doped maghemite (γ-Fe_2O_3) NPs with 25 kDa branched PEI (PEI_{25}) and (ii) a final NP/PEI_{25} shell-controlled oxidation using aqueous H_2O_2 as oxidant (Figure 1).

PEI_{25}-Decorated CAN-γ-Fe_2O_3 Nanoparticles (PEI_{25}-CAN-γ-Fe_2O_3 NPs). 1.0 mL of an aqueous suspension of ultrasmall $Ce^{3/4+}$-doped maghemite (γ-Fe_2O_3) NPs (CAN-γ-Fe_2O_3 NPs, ICP-AES measurements: Fe: 3.88 mg/mL − 3.88 mg total Fe, 0.0696 mmol Fe) were prepared by as previously described[16,17] was diluted to 28.0 mL using Milli-Q-purified H_2O. Then, 20.136 mg of 25 kDa branched PEI (0.0008 mmol, PEI/Fe Wt ratio: 5.25) was added at room temperature to the NP suspension as an aqueous solution (10.0 mg PEI_{25}/ml) and the suspension was shaken overnight at room temperature (RT) (orbital shaker). Following this reaction, the resulting crude PEI_{25}-CAN-γ-Fe_2O_3 NPs were washed 3 times (3 × 10 mL ddH_2O) using an Amicon Ultra-15 centrifugal filter device (100 K) operated at 4000 rpm (12 min) followed by a size exclusion process performed using centrifugation (8000 rpm/min, 16 min, 18 °C, and 7000 rpm, 10 min, 18 °C) to yield cleaned PEI_{25}-CAN-γ-Fe_2O_3 NPs.

Controlled H_2O_2-Mediated PEI_{25} Shell Oxidation of PEI_{25}-CAN-γ-Fe_2O_3 NPs toward Corresponding $PEI_{25\text{-}ox}$-CAN-γ-Fe_2O_3 NPs (MagRET NPs). In a typical PEI_{25}-modifying oxidation reaction, 3.1 mL of the aqueous suspension of PEI_{25}-CAN-γ-Fe_2O_3 (ICP-AES measurement: Fe = 0.41 mg/mL, Fe = 1.0664 mg, NPs concentration: 4.1 mg NPs/mL) was further diluted to 14.0 mL (ddH_2O) in a conical plastic centrifuge tube. Then, 0.341 mL of an aqueous 0.000075 wt % solution of H_2O_2 in Milli-Q-purified H_2O was added (0.1% of PEI_{25}-CAN-γ-Fe_2O_3 NP primary amine (NH_2) moles as assayed by a ninhydrin-based Kaiser testing[46] − 0.0008 mmol NH_2/mg NPs) and the reaction mixture shaken overnight (250 rpm, 10 °C) using a cooled orbital shaker. The resulting reaction mixture was then washed by Milli-Q-purified H_2O (3 × 8 mL) using an Amicon Ultra-15 centrifugal filter device (100 K) operated at 4000 rpm (centrifuge) for 5−6 min (RT, 18 °C), and then further concentrated to a 0.5−1 mL NP suspension by water vacuum evaporation (ICP-AES measurement: Fe = 0.41 mg/mL).

Dipicolinic Acid Ligand "Saturation" Experiment. CAN-γ-Fe_2O_3 NPs (3.20 mg NPs, 1.77 mg elemental Fe/ICP-AES) have been first reacted with a specific tridentate dipicolinic acid ligand in excess (0.1 mg, 0.598 μmol, ddH_2O, 3 days, 20 °C) following by a cleaning step (sequential centrifugal NP precipitation-redispersion, ddH_2O washings, 3×). Then, Dpic-modified CAN-γ-Fe_2O_3 NPs (0.2 mL, 0.70 mg elemental Fe/ICP-AES) have been similarly contacted with a known excess amount of fluorescent FITC-labeled PEI_{25} polymer (FITC-PEI_{25}/DMSO, 0.12 mg, 0.0048 μmol, ddH_2O, overnight, 20 °C) followed by extensive NP cleaning (sequential centrifugal precipitation and NP redispersion, ddH_2O washings, 3×). Finally, the resulting washing phase fluorescence was measured (UV absorption quantification using FITC fluorescence signal, λ_{max} = 495 nm, extinction coefficient: 75 000 M^{-1} cm^{-1}).

Cell Lines and Culture. BxPC-3 human pancreatic adenocarcinoma and SK-OV-3 human ovarian adenocarcinoma cells were obtained from the American Type Culture Collection (ATCC). Human megakaryoblastic (CMK) leukemia cells were obtained from the German Collection of Microorganisms and Cell Cultures (DSMZ, Braunschweig, Germany). The dual luciferase-expressing U2OS human osteosarcoma cell line was generated as previously described[47] and enzyme activities of the *Renilla* and *Firefly* luciferases were determined using Dual-Luciferase Assay System (Promega). All cells were cultured in Dulbecco's Modified Eagle Medium or RPMI-1640 medium and grown at 37 °C in a 5% CO_2 atmosphere.

Penetration of MagRET NPs to SK-OV-3 Cells. Cells were seeded in a 12 well plate (Greiner) with coverslips and incubated overnight at 37 °C with 5% CO_2. Cells were transfected with siGLO Green Transfection Indicator (50 nM) (FITC) (Dharmacon) mixed with MagRET NPs at a 0.315 Fe/siRNA w/w ratio. After 24 h, lysosomes were stained with Lysotracker (Cy3) (Life Technologies) for 30 min at 37 °C following manufacturer protocol, then cells were fixed with Paraformaldehyde solution (4% in PBS) (Santa Cruz Biotechnology) for 20 min at RT, and nuclei were stained with DAPI solution (1 μg/mL in PBS) (blue) (Sigma) for 10 min at RT. Images were taken with a Leica TCS SPE (X63)

DOI: 10.1021/acs.bioconjchem.5b00276
Bioconjugate Chem. 2015, 26, 1692−1701

Confocal Laser Scanning Microscope (CLSM), and then, the 3D images were edited in the software Imaris (Bitplane).

Silencing Experiments. Cells were seeded in a 6, 12, or 96 well plate and incubated overnight at 37 °C with 5% CO_2. Cells were transfected with different siRNAs (see Supporting Information Table S1 for siRNA details) mixed with MagRET NPs at a 0.315 Fe/siRNA w/w ratio. After incubation, cells, proteins, or total RNA were isolated for further analysis.

MTT Assay. Cells were seeded in a 96 well plate (Greiner) and incubated overnight at 37 °C with 5% CO_2. Cells were treated with different concentrations of MagRET NPs (determined by iron concentrations) or without NPs (control), and then incubated for 72 h at 37 °C with 5% CO_2. MTT assay (Sigma) was performed according to the manufacturer's instructions.

Western Blot Analysis. Cells were lysed, and proteins were extracted. Proteins were separated on either 8% or 10% SDS-polyacrylamide gel and reacted with antibodies (see Supporting Information Table S2 for antibodies details).

qPCR of mRNAs and miRNAs. Total RNA was isolated with TRI Reagent (Sigma) and RNA quality and quantity were determined with a spectrophotometer (Nanodrop 1000, Fisher Scientific). cDNA was prepared using First Strand cDNA Synthesis Kit (Thermo). qPCR was performed using the Fast SYBR Green Master Mix and the StepOnePlus Real-Time PCR System (Applied Biosystems). For determining the microRNA levels TaqMan MicroRNA Assay and TaqMan MicroRNA RT kits were used (Applied Biosystems) (see Supporting Information Table S3 for primer details).

Cell Cycle and Caspase 3/7 Activity Analyses. Cells were fixed with cold ethanol at 4 °C overnight. Before analysis, fixed cells were washed and resuspended in 1 mL of PBS containing 200 μg/mL RNase A (10−109−169, Roche Applied Science) and 5 μg/mL propidium iodide (P4170, Sigma-Aldrich, St. Louis, MO, USA). After incubation for 20 min at 37 °C, cells were analyzed for DNA content by flow cytometry (Gallios, Beckman Coulter). For each sample, 10 000 events were acquired and cell cycle distribution was determined using cell cycle analysis software (ModFit LT).

Caspase 3/7 activities were determined using Caspase-Glo 3/7 Assay system (Promega).

In Vivo Experiments. All animal experiments were performed in compliance with the Guidelines for the Care and Use of Research Animals established by the Bar-Ilan University Animal Studies Committee. BALB/c mice (Harlan Laboratories Israel Ltd., Jerusalem, Israel) aged 8−9 weeks were injected intravenously with CAN-γ-Fe_2O_3 (0.315 mg/kg), PEI_{25}-CAN-γ-Fe_2O_3 (0.315 mg/kg), or $PEI_{25\text{-}OX}$-CAN-γ-Fe_2O_3 (0.315 mg/kg) (MagRET) NPs or saline. Each group was composed of 6 mice. Toxicity was assessed by mortality within 24 h of NP injection.

Statistical Analyses. Statistical analysis of the data was performed with the GraphPad Prism software (GraphPad Software).

■ ASSOCIATED CONTENT

Ⓢ Supporting Information

siRNA and primer sequences for silencing experiments and RT-PCR analyses. Antibody details for Western blot analysis. siRNA adsorption results by MagRET NPs. Superimposed FTIR spectra of both starting and of dipicolinic acid-decorated CAN-γ-Fe_2O_3 NPs. FTIR analyses of PEI_{25} oxidation reactions. This material is available free of charge via the Internet at http://pubs.acs.org/.The Supporting Information is available free of charge on the ACS Publications website at DOI: 10.1021/acs.bioconjchem.5b00276.

■ AUTHOR INFORMATION

Corresponding Authors

*E-mail: jean-paul.m.lellouche@biu.ac.il. Tel: 972-3-5318324. Fax: 972-3- 7384053.

*E-mail: michaes@mail.biu.ac.il. Tel: 972-3-5318068. Fax: 972-3-5318124.

Author Contributions

#E. Lellouche and L. L. Israel contributed equally to this work.

Notes

The authors declare no competing financial interest.

■ ACKNOWLEDGMENTS

This work was supported in part by a grant from the Israeli National Nanotechnology Initiative in the Focal Technology Area: Nanomedicines for Personalized Theranostics, and the I-core grant 40/11 from the Israel Science Foundation. Funding by both (i) the VIIth Framework RTD European Project (FP7-NMP-2010-LARGE-4 area) - Large Collaborative Project SaveMe (grant agreement no 263307), and (ii) the Israel Ministry of Industry & Trade (KAMIN & Magnet RIMONIM projects) is gratefully acknowledged.

■ REFERENCES

(1) Kanasty, R., Dorkin, J. R., Vegas, A., and Anderson, D. (2013) Delivery materials for siRNA therapeutics. *Nat. Mater. 12*, 967−977.

(2) Lee, J. M., Yoon, T. J., and Cho, Y. S. (2013) Recent developments in nanoparticle-based siRNA delivery for cancer therapy. *BioMed. Res. Int. 2013*, 1−10.

(3) Dominska, M., and Dykxhoorn, D. M. (2010) Breaking down the barriers: siRNA delivery and endosome escape. *J. Cell Sci. 123*, 1183−1189.

(4) Wahajuddin, and Arora, S. (2012) Superparamagnetic iron oxide nanoparticles: magnetic nanoplatforms as drug carriers. *Int. J. Nanomed. 7*, 3445−3471.

(5) Wu, C., Gong, F., Pang, P., Shen, M., Zhu, K., Cheng, D., Liu, Z., and Shan, H. (2013) An RGD-modified MRI-visible polymeric vector for targeted siRNA delivery to hepatocellular carcinoma in nude mice. *PLoS One 8*, e66416.

(6) Esteller, M. (2011) Non-coding RNAs in human disease. *Nat. Rev. Genet. 12*, 861−874.

(7) Kanasty, R. L., Whitehead, K. A., Vegas, A. J., and Anderson, D. G. (2012) Action and reaction: the biological response to siRNA and its delivery vehicles. *Mol. Ther. 20*, 513−524.

(8) Kang, S., Im, K., Baek, J., Yoon, S., and Min, H. (2014) Macro and small over micro: macromolecules and small molecules that regulate microRNAs. *ChemBioChem 15*, 1071−1078.

(9) Spizzo, R., Nicoloso, M. S., Croce, C. M., and Calin, G. A. (2009) SnapShot: MicroRNAs in Cancer. *Cell 137*, 586−586.e581.

(10) Griveau, A., Bejaud, J., Anthiya, S., Avril, S., Autret, D., and Garcion, E. (2013) Silencing of miR-21 by locked nucleic acid-lipid nanocapsule complexes sensitize human glioblastoma cells to radiation-induced cell death. *Int. J. Pharm. 454*, 765−774.

(11) Liu, X. Q., Song, W. J., Sun, T. M., Zhang, P. Z., and Wang, J. (2011) Targeted delivery of antisense inhibitor of miRNA for antiangiogenesis therapy using cRGD-functionalized nanoparticles. *Mol. Pharmaceutics 8*, 250−259.

(12) Liu, X., Li, G., Su, Z., Jiang, Z., Chen, L., Wang, J., Yu, S., and Liu, Z. (2013) Poly(amido amine) is an ideal carrier of miR-7 for enhancing gene silencing effects on the EGFR pathway in U251 glioma cells. *Oncol. Rep. 29*, 1387−1394.

DOI: 10.1021/acs.bioconjchem.5b00276
Bioconjugate Chem. 2015, 26, 1692−1701

(13) Su, J., Baigude, H., McCarroll, J., and Rana, T. M. (2011) Silencing microRNA by interfering nanoparticles in mice. *Nucleic Acids Res. 39*, e38.
(14) Hauptman, N., and Glavač, D. (2013) Long non-coding RNA in cancer. *Int. J. Mol. Sci. 14*, 4655−4669.
(15) Gutschner, T., Hämmerle, M., and Diederichs, S. (2013) MALAT1 – a paradigm for long noncoding RNA function in cancer. *J. Mol. Med. (Heidelberg, Ger.) 91*, 791−801.
(16) Israel, L. L., Buchman, K., Lellouche, E., Michaeli, S., and Lellouche, J.-P. (2014) pp 1−66, University Bar-Ilan, Israel.
(17) Haviv, A. H., Grenèche, J. M., and Lellouche, J. P. (2010) Aggregation control of hydrophilic maghemite (gamma-Fe_2O_3) nanoparticles by surface doping using cerium atoms. *J. Am. Chem. Soc. 132*, 12519−12521.
(18) Massart, R., Dubois, E., Cabuil, V., and Hasmonay, E. (1995) Preparation and properties of monodisperse magnetic fluids. *J. Magn. Magn. Mater. 149*, 1−5.
(19) Israel, L. L., Lellouche, E., Kenett, R. S., Green, O., Michaeli, S., and Lellouche, J.-P. (2014) $Ce^{3/4+}$ cation-functionalized maghemite nanoparticles towards siRNA-mediated gene silencing. *J. Mater. Chem. B 2*, 6215−6225.
(20) Aghabozorg, H., Roshan, L., Firoozi, N., Bagheri, S., Ghorbani, Z., Kalami, S., Mirzaei, M., Shokrollahi, A., Ghaedi, M., Aghaei, R., et al. (2010) Syntheses, crystal, and molecular structures of Mn(II), Zn(II), and Ce(III) compounds and solution studies of Mn(II), Ni(II), Cu(II), Zn(II), Cd(II), and Ce(III) compounds obtained from a suitable proton transfer compound containing bda and pydcH2 (bda = butane-1,4-diamine; pydcH2 = pyridine-2,6-dicarboxylic acid). *Struct. Chem. 21*, 701−714.
(21) Prasad, T. K., and Rajasekharan, M. V. (2005) A novel water octamer in $Ce(dipic)_2(H_2O)_3{\cdot}4H_2O$: crystallographic, thermal, and theoretical studies. *Cryst. Growth Des. 6*, 488−491.
(22) Katada, H., Seino, H., Mizobe, Y., Sumaoka, J., and Komiyama, M. (2008) Crystal structure of Ce(IV)/dipicolinate complex as catalyst for DNA hydrolysis. *J. Biol. Inorg. Chem. 13*, 249−255.
(23) Kim, J.-H., Lee, S., Kim, K., Jeon, H., Park, R.-W., Kim, I.-S., Choi, K., and Kwon, I. C. (2007) Polymeric nanoparticles for protein kinase activity. *Chem. Commun. (Cambridge, U. K.)*, 1346−1348.
(24) Sjöback, R., Nygren, J., and Kubista, M. (1995) Absorption and fluorescence properties of fluorescein. *Spectrochim. Acta, Part A 51*, L7−L21.
(25) Hobel, S., and Aigner, A. (2013) Polyethylenimines for siRNA and miRNA delivery in vivo. *Wiley Interdiscip. Rev.: Nanomed. Nanobiotechnol. 5*, 484−501.
(26) Moghimi, S. M., Symonds, P., Murray, J. C., Hunter, A. C., Debska, G., and Szewczyk, A. (2005) A two-stage poly(ethylenimine)-mediated cytotoxicity: implications for gene transfer/therapy. *Mol. Ther. 11*, 990−995.
(27) Ottaviano, A. J., Sun, L., Ananthanarayanan, V., and Munshi, H. G. (2006) Extracellular matrix-mediated membrane-type 1 matrix metalloproteinase expression in pancreatic ductal cells is regulated by transforming growth factor-beta1. *Cancer Res. 66*, 7032−7040.
(28) Dangi-Garimella, S., Krantz, S. B., Barron, M. R., Shields, M. A., Heiferman, M. J., Grippo, P. J., Bentrem, D. J., and Munshi, H. G. (2011) Three-dimensional collagen I promotes gemcitabine resistance in pancreatic cancer through MT1-MMP-mediated expression of HMGA2. *Cancer Res. 71*, 1019−1028.
(29) Degenhardt, Y., and Lampkin, T. (2010) Targeting Polo-like kinase in cancer therapy. *Clin. Cancer Res. 16*, 384−389.
(30) Riedl, S. J., and Salvesen, G. S. (2007) The apoptosome: signalling platform of cell death. *Nat. Rev. Mol. Cell Biol. 8*, 405−413.
(31) Luo, X., and Kraus, W. L. (2012) On PAR with PARP: cellular stress signaling through poly(ADP-ribose) and PARP-1. *Genes Dev. 26*, 417−432.
(32) Mellott, A. J., Forrest, M. L., and Detamore, M. S. (2013) Physical non-viral gene delivery methods for tissue engineering. *Ann. Biomed. Eng. 41*, 446−468.
(33) Komatsu, N., Suda, T., Moroi, M., Tokuyama, N., Sakata, Y., Okada, M., Nishida, T., Hirai, Y., Sato, T., and Fuse, A. (1989) Growth and differentiation of a human megakaryoblastic cell line, CMK. *Blood 74*, 42−48.
(34) Yang, Y., Qian, J., Chen, Y., and Pan, Y. (2014) Prognostic role of circulating microRNA-21 in cancers: evidence from a meta-analysis. *Tumor Biol. 35*, 6365−6371.
(35) Gutschner, T., Hämmerle, M., Eissmann, M., Hsu, J., Kim, Y., Hung, G., Revenko, A., Arun, G., Stentrup, M., Gross, M., et al. (2013) The noncoding RNA MALAT1 is a critical regulator of the metastasis phenotype of lung cancer cells. *Cancer Res. 73*, 1180−1189.
(36) Yang, F., Yi, F., Han, X., Du, Q., and Liang, Z. (2013) MALAT-1 interacts with hnRNP C in cell cycle regulation. *FEBS Lett. 587*, 3175−3181.
(37) Qiu, M. T., Hu, J. W., Yin, R., and Xu, L. (2013) Long noncoding RNA: an emerging paradigm of cancer research. *Tumor Biol. 34*, 613−620.
(38) Karraker, D. G. (1970) Coordination of trivalent lanthanide ions. *J. Chem. Educ. 47*, 424−430.
(39) Limaye, S. N., and Saxena, M. C. (1986) Relative complexing tendencies of O—O, O—N, and O—S donor (secondary) ligands in some lanthanide−EDTA mixed-ligand complexes. *Can. J. Chem. 64*, 865−870.
(40) Arnold, P. L., Casely, I. J., Zlatogorsky, S., and Wilson, C. (2009) Organometallic cerium complexes from tetravalent coordination complexes. *Helv. Chim. Acta 92*, 2291−2303.
(41) Aghabozorg, H., Sadr-khanlou, E., Shokrollahi, A., Ghaedi, M., and Shamsipur, M. (2009) Synthesis, characterization, crystal structures, and solution studies of Ni(II), Cu(II) and Zn(II) complexes obtained from pyridine-2,6-dicarboxylic acid and 2,9-dimethyl-1,10-phenanthroline. *J. Iran. Chem. Soc. 6*, 55−70.
(42) Edelmann, F. T. (2012) Lanthanides and actinides: Annual survey of their organometallic chemistry covering the year 2009. *Coord. Chem. Rev. 256*, 1151−1228.
(43) Harel-Bellan, A., Zazoua, M. A., Rachez, C., Muchardt, C., and Batsché, E. (2013) 10-million-years AGO: Argonaute on chromatin in yeast and human, a conserved mode of action? *Transcription 4*, 89−91.
(44) Robb, G. B., Brown, K. M., Khurana, J., and Rana, T. M. (2005) Specific and potent RNAi in the nucleus of human cells. *Nat. Struct. Mol. Biol. 12*, 133−137.
(45) Gagnon, K. T., Li, L., Chu, Y., Janowski, B. A., and Corey, D. R. (2014) RNAi factors are present and active in human cell nuclei. *Cell Rep. 6*, 211−221.
(46) Sarin, V. K., Kent, S. B., Tam, J. P., and Merrifield, R. B. (1981) Quantitative monitoring of solid-phase peptide synthesis by the ninhydrin reaction. *Anal. Biochem. 117*, 147−157.
(47) Buchman, Y. K., Lellouche, E., Zigdon, S., Bechor, M., Michaeli, S., and Lellouche, J. P. (2013) Silica nanoparticles and polyethyleneimine (PEI)-mediated functionalization: a new method of PEI covalent attachment for siRNA delivery applications. *Bioconjugate Chem. 24*, 2076−2087.

DOI: 10.1021/acs.bioconjchem.5b00276
Bioconjugate Chem. 2015, 26, 1692−1701